



Multiaxial fatigue of in-service aluminium longerons for helicopter rotor-blades

A. Shanyavskiy

State Center for Civil Aviation Flight Safety, Airport Sheremetievo-1, PO Box 54, Chimkinskiy State, Moscow region, 141426, Russia,

106otdel@mail.ru, http://orcid.org/0000-0001-2345-6789

A. Toushentsov

State Center for Civil Aviation Flight Safety, Airport Sheremetievo-1, PO Box 54, Chimkinskiy State, Moscow region, 141426, Russia,

103otdel@mail.ru, http://orcid.org/0000-0002-2345-6790

ABSTRACT. Fatigue cracking of longerons manufactured from Al-alloy AVT-1 for helicopter in-service rotor-blades was considered and crack growth period and equivalent of tensile stress for different blade sections were estimated. Complicated case of in-service blades multiaxial cyclically bending-rotating and tension can be considered based on introduced earlier master curve constructed for aluminum alloys in the simple case of uniaxial tension with stress R-ratio near to zero. Calculated equivalent tensile stress was compared for different blade sections and it was shown that in-service blades experienced not principle difference in this value in the crack growth direction by the investigated sections. It is not above the designed equivalent stress level. Crack growth period estimation in longerons based on fatigue striation spacing or meso-beach-marks measurements has shown that monitoring system introduced designer in longerons can be effectively used for in-time crack detecting independently on the failed section when can appeared because of various type of material faults or in-service damages.

KEYWORDS. Fatigue; Multiaxial; Longerons; Aluminium alloy; Crack growth; Fractography; Stress equivalent.

INTRODUCTION

Fatigue cracking of longerons manufactured from Al-alloy AVT-1 for helicopter in-service rotor-blades was considered and crack growth period and equivalent of tensile stress for different blade sections were estimated. Complicated case of in-service blades multiaxial cyclically bending-rotating and tension can be considered based on introduced earlier master curve constructed for aluminum alloys in the simple case of uniaxial tension with stress R-ratio near to zero [1]. Calculated equivalent tensile stress was compared for different blade sections and it was shown that in-service blades experienced not principle difference in this value in the crack growth direction by the investigated sections. It is not above the designed equivalent stress level. Crack growth period estimation in longerons based on fatigue striation spacing or meso-beach-marks measurements has shown that monitoring system introduced designer in longerons can be

effectively used for in-time crack detecting independently on the failed section when can appeared because of various type of material faults or in-service damages.

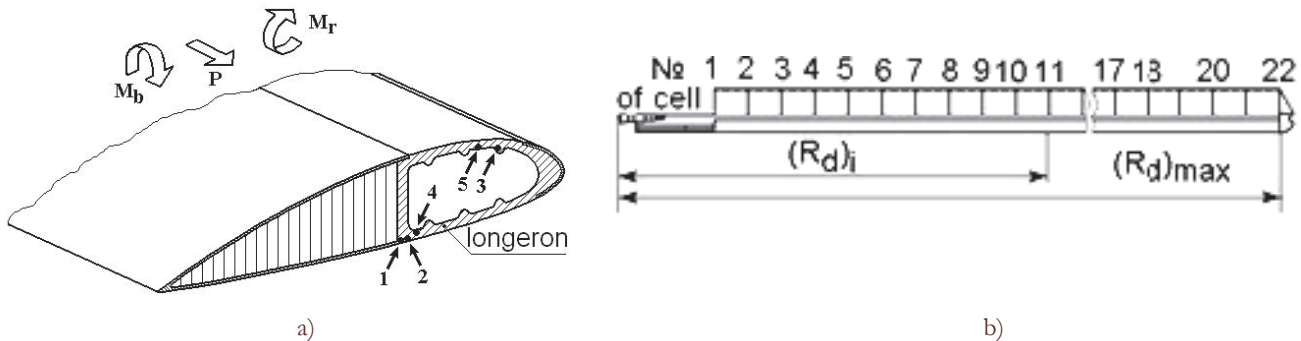


Figure 1: Scheme (a) of rotor-blade section with numbering “1”-“5” areas for crack origination and pointed out its external loading and (b) cells position for a blade.

The pressure gage, installed in the basement portion of the rotor blade, is designed to send a signal of lost excessive pressure to a monitor (a window in that a watcher can see the red cup to appear) once discontinuity arose in the longeron in any section of the propeller blade. According to the service norms, such inspection is to be performed each time before the flight.

In-service fatigue cracks nucleated in the longerons in the defect sites that were revealed all over the blade length, from $\bar{R} = 0.085$ to $\bar{R} = 0.71$, where $\bar{R} = (R_d)_i / (R_d)_{\max}$ (see Fig. 1b).

In the paper we shall discuss in details the fracture trends of the longerons made of aluminium AVT-1 alloy.

INSPECTION RESULTS OF FATIGUE-CRACKING BEHAVIOR OF THE LONGERONS

Fatigue cracks only nucleated in operating longerons of the rotor-blades if their material was somehow damaged [2, 3]. Despite the fact that the defects differed in the sites of location in the cross-section area of the longeron (see Fig. 1), all the defects caused failure of the fatigue nature. We can formalize these failure cases according to a general scheme of the fracture surface, Fig. 2, as composed of:

- a fracture-origin exhibits a fracture relief typical of the damage kind and may be located anywhere on the inner or outer surface of the longeron walls;
- a zone (1) of stable crack growth typically exhibits a smooth fracture surface with distinct mesoscopic or macroscopic (depending of the fracture location) beach-marks of fatigue fracture;
- a zone (2) of accelerated crack propagation typically shows a wavy fracture surface of the “Christmas-tree” or “chevron-like” type;

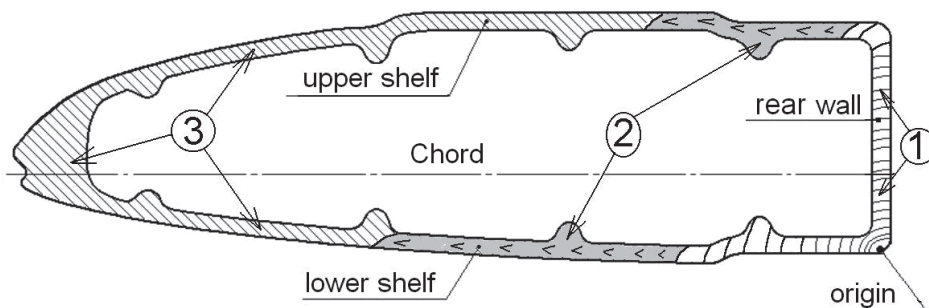


Figure 2: Scheme of longerons fracture surfaces for crack origination from the corrosion pitting with indication “1”-“3” different fracture surface areas.



- a zone (3) of fast crack propagation when the plastic-shear lips form entirely over the wall-thickness of the longeron. In the zone 1, pseudo-striations pattern forms first (P-region), peculiar to low-rate crack growth in the near-threshold range of the kinetic diagram. The material here experiences extensive shear. As the crack length increases, a pattern of fatigue striations forms or, alternatively, mesoscopic fatigue beach-marks dominate, depending on the blade section in that the crack propagates.

Formation of fatigue striations alternating with dimpled fracture is typical of the zone 2: here, the crack growth becomes accelerated.

Purely dimpled relief is typical of the zone 3 of final fracture; here the plastic-shear lips form throughout an entire thickness of the blade wall.

Having fatigue meso-beach-marks and fatigue striations distinctly visible made it possible to analyze the growth trends of fatigue cracks in the longerons and to determine the growth durations of the cracks and estimate the in-service stress level. Furthermore, it made possible to verify if the crack-monitoring alarm gage, installed, by design, in the longeron-basement end, operated efficiently.

Consider the data on two cases; in one case the crack was disclosed as it grew not above 25% of the total cross-section area of the longeron and in the other case the longeron failed in flight as the crack occupied 75% of its cross-section. The two helicopters were of the same type and the fracture sites almost coincided. The cases appeared contradicting to one another, i.e., indicated both to the efficient and inefficient operation of the alarm gage. Moreover, that fatigue zone, which amounted in total to 25-% of the cross-section of the longeron, occupied equal areas on both sides (top and bottom) of the neutral bending line. Consequently, the longeron had the crack partially closed in the qualitatively similar ways whether in flight or in the parked condition. Still the gage responded to the drop of pressure in both conditions, which showed its sensitivity as quite high. In such a contradictory situation, when cracks were now revealed and now not revealed, one had to either improve the gage efficiency or discipline the inspecting organizations to use the gage carefully.

One could estimate the gage efficiency most correctly using the data on growth duration of fatigue cracks and in-service stresses as applied to the separate blade sections. In so doing, one first should examine the crack-growth patterns in the longerons subjected to bench tests simulating various loading conditions. Secondly, one should see to which degree the propagation patterns of fatigue cracks remain similar in the separate longeron sections.

INITIATION AND PROPAGATION PATTERNS OF FATIGUE CRACKS IN SERVICE

Blades in flight are loaded with the frequency that is determined by the revolution frequency of the rotor and corresponds to the frequency of the single cycles of fatigue damage. Accordingly, we calculate the growth period of fatigue cracks based on the measurements of fatigue-striation spacing and assuming that each single fatigue striation is formed as a result of one rotor revolution. This consideration of material damage has accordance with longerons fatigue tests on the special test-device that were performed earlier [2]. We shall compare below these estimations with the crack-growth durations calculated based on the data on fatigue meso-beach-marks (MBM).

The area of early crack growth, with typically P-region of fracture, was the largest in the damage site, in the section of relative radius $\bar{R} = 0.085$ (beside the blade basement); it measured about 25 mm in length. In all the other sections such crack-growth areas were smaller, though no relation between the fracture region size and the relative radius of a longeron was revealed.

For the separate longeron sections (distances from the blade basement), the growth periods of fatigue cracks were estimated based on the data on the fatigue-meso-beach-marks and fatigue-striation spacings. In the region of relative radius $\bar{R} = 0.085$ of the longeron fatigue MBM were characteristic of the fatigue damage all over the crack path from the fracture-origin site till the transition to unstable crack growth. This fatigue fracture was initiated owing to the preliminary corrosion cracking of the material.

Beyond the fracture-origin area MBM geometry is perfect and the meso-beach-mark spacing increases regularly in the crack-growth directions. Fatigue striations began to form as the crack increased to 25 mm along the rear wall. Plus to them, meso-beach-marks continued to form clearly, which helped to estimate with greater accuracy the crack-growth duration over both in the striation-free (P-region) and striation-bearing portions of the fracture.

Immediately before the fast-cracking zone began, MBM formed as distinctly as to be visible at quite moderate magnifications (with the use of a light microscope), indicating to quite heavy fatigue damage. We may say that these coarse (macroscopic) fatigue lines formed to respond to the effects of regularly altered applied loads. By the end-rupture time the fatigue crack passed through 45% portion of the longeron cross-section. In these limits (from the origin site till end-rupture zone), the crack grew by 120 mm along the bottom wing and by 52 mm along the rear wall.

Sequentially measured distances between MBM and, then, between the Macro-Beach-Marks confirmed that there recurrence along the crack path is not casual, but regular, indicative of the very blade-loading patterns, regularly repeated with each single flight cycle, Fig. 3. Therefore, the regularly increasing distances between these marks are indicative of the crack-growth rate regularly increasing from flight to flight. And the number of these beach-marks corresponds to the number of the helicopter flights accomplished with the fatigue crack propagating in the longeron.

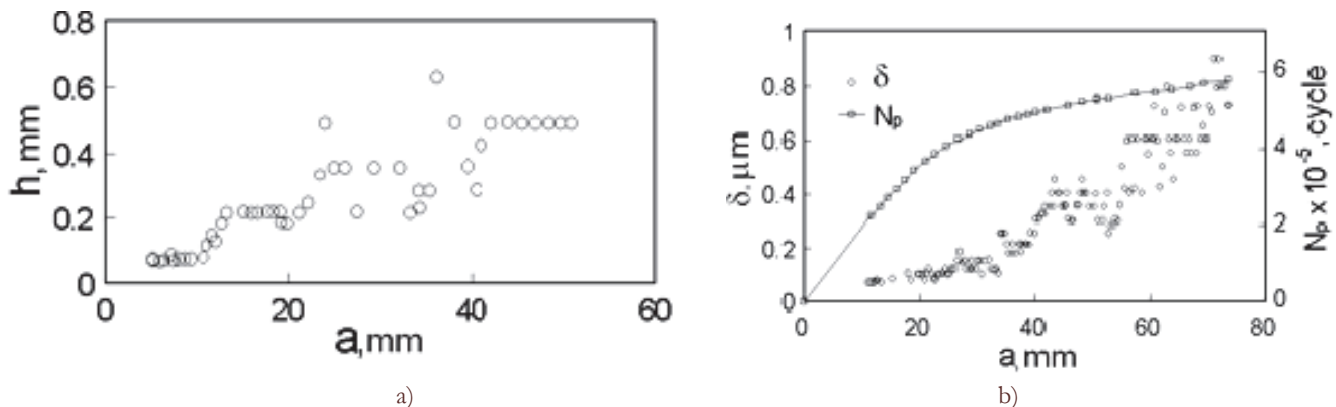


Figure 3: Spacing of (a) meso- or macro-beach-marks and (b) fatigue striations with number of cycles N_p against crack length a for two longerons (a) and (b).

In case that the distances between the fatigue beach-marks remain unchanged for some periods of crack propagation shows the crack-length increments to obey some scale hierarchy both at the mesoscopic (MBM or fatigue striations) and macroscopic levels. This particular trend again indicates that the blades were loaded in a regular way (each single flight); the latter showed itself through the pattern of regularly advancing fatigue crack.

Fatigue MBM were counted starting from the area 5.5 mm apart from the crack-origin site (the lines became most distinct here) to find out that the following crack-growth period involved about 210 flights. The inter-MBM distances (and, hence, the crack-length increments) appeared to sequentially increase. For the crack length grown from 5.5 to 7 mm, the average length increment did not exceed 0.056 mm per flight. So, not less than 70 flights were done with the fatigue crack growing in length from 1.5 to 5.5 mm. The starting crack length of 1.5 mm was taken a little greater than the depth (1.3 mm) of the stress-corrosion-origin. In total, these estimations give 280 (210 + 70) flight cycles for the period of crack propagation from the corrosion-cracking zone till the beginning point of unstable fracture.

Of the considered cases of the failure of longerons, the fracture at the site of $R = 0.7$ related to the cases of the deepest fatigue cracks: here, the P-region of early cracking measured as much as 12 mm. The blade fracture began from a nearly spherical cavity as large as about 2 mm in radius, located at the inner surface of the longeron. On both sides of the crack, cavities, similar to the cavity from which the fracture began, were arranged in a file along the longeron axis.

The value of striation spacing increased with the crack length in a way indicative of the regular loading pattern of the longeron in service. The spacing of fatigue striations irregularly increasing and decreasing with increasing crack length only appeared immediately before the transition to accelerated crack growth and a chevron-like fracture morphology (see number "2" on Fig. 2). The calculations were done according to the following relationships [1, 4].

In so doing, 57000 cycles was thus calculated for crack-growth period in P-region. In average, single-flight duration is close to 30 minutes, and a loading frequency is determined by the revolution frequency (192 revolutions per minute) of the rotor. Consequently, the crack growth duration in the longeron must be not less than 49.5 hours (about 100 flights). These figures do not contradict the macroscopic view of the fracture morphology. Using a binocular microscope at small magnifications, one could observe indistinct fatigue macro-beach-marks in individual parts of the fracture. Such marks were used for estimating the flight number, which then was compared with the flight number acquired from the fatigue-striation patterns. The two estimations appeared to differ not more than by 10%.

Therefore, using predominantly the patterns of MBM and fatigue striations we may estimate the growth durations of fatigue cracks. Having compared these estimations, we may see that cracks of fatigue nature grow in the longerons for quite long periods and, hence, inspection and monitoring of their growth in service can be highly efficient.



LEVELS OF EQUIVALENT STRESS IN THE LONGERONS OF MI-4 AND MI-8 HELICOPTERS

From the above data one can see that propagation of fatigue cracks in the longerons takes quite a long time. This information, however, should be enlarged to answer how much descriptive are the usually applied calculation methods as concerns the actual stress-strain conditions of the material in various sections of a longeron. Having this question answered is especially important, as corrosion-induced damage is well known to occur and, sometimes, be a source of fatigue cracks in the longerons.

Let us discuss the levels of equivalent stress σ_e with respect to various relative radii of the longerons; the stress levels are estimated in terms of the concept of the single kinetic curve with the use of above-described quantitative-fractography approach to the failure cases of aviation structures.

Along the longeron, the stress level changes with the distance from the longeron basement. Tensile stress diminishes and, simultaneously, bending load increases. This complex loading pattern results in stresses that vary in the level and in the ratio between the torsion and bending components. Longerons experience a permanent tensile stress, whose largest value is 60 MPa, and the stress that varies between 10 MPa and 38 MPa. In flight, a longeron is twisted within 3° , and the torsion stress achieves 30 MPa.

As follows from the analysis of stressed state of the specimens loaded simultaneously by torsion and tension [5], crack-growth behavior is predominantly controlled by the value of crack opening normal to the crack-growth direction. In other words, a crack propagates along the normal to the axis of maximum tensile stress, applied to the crack tip. Typically, crack-propagation occurs with fatigue striations forming in the fracture area. Therefore, we can estimate a crack-growth rate using a synergetic approach, based on the concept of master kinetic curve [1, 4]. Striations do not appear in case of out-of-phase loading [6], when the cycle asymmetry R near to zero.

Though caused by combined uniaxial tension and torsion, fatigue fracture develops as a single phenomenon. Therefore, a unified energetic criterion was proposed [6] for describing fatigue-cracking behavior under such combined tension-and-torsion conditions. Making use of that criterion helps the calculation of a tension equivalent for stress-intensity factor K_e from the following relationships.

$$K_e = K_I (1 - C_{II} \lambda_\sigma^2 + C_{III} \lambda_\tau^2)^{1/2} \quad (1)$$

In Eq. (3) dimensionless coefficients C_{II} and C_{III} only depend on the Poisson's ratio and characterize the effects of the crack-opening modes K_{II} and K_{III} for a pipe-type specimen twisted in the crack plane. Eq. (3) relates to the case of using the master curve of fatigue-cracking kinetics for various combinations of shear and tensile components of torsion-and-tension loading. Here the equivalent stress-intensity factor appears a quantity only dependent on a correction $F(\omega)$ for a torsion angle, ω , which value was calculated, typical of all the other cases, for the master kinetics curve [1, 4, 6].

A loading pattern of the rotor-blades repeats quite regularly every flight. So, statistically, we can discuss crack-growth events in various blade sections as relating to the same loading type. The levels of equivalent stress were estimated for various sections and origin sites of fatigue cracks. Below, we illustrate the methodological principles of these calculations for the case of fatigue-crack growth at the relative radius $\bar{R} = 0.38$ of a longeron.

In this section, stresses to be calculated arise from varying stresses and dynamic tension of 59 MPa. In such a case an equivalent stress can be estimated from a relationship

$$\sigma_e = \sigma_{\max} \sqrt{(1 - \sigma_{\min}/\sigma_{\max})} = 81.5 \sqrt{(1 - 0.45)} = 60.5 \quad (2)$$

From the laboratory tests of AVT3-1 alloy the value of $K_{Ip} = 7.9 \text{ MPa m}^{1/2}$ was acquired for border transition from P-region to the stage of fatigue striation formation. For the longeron of interest, this value is achieved as the crack reaches 6 mm in length. And using a respective relationship [7], we may estimate a stress-intensity factor for a round crack as

$$K_{Ip} = \sigma_e \sqrt{\pi a_0} / \Phi, \quad (3)$$

where $\Phi \approx 1$.



From Eq. (3) we found the equivalent stress $\sigma_e = 58$ MPa for the crack length $a_0 = 6$ mm. One can see that loading conditions remained the same and no positive or negative deviation occurred from the equivalent-stress level all over the fatigue-striation stage.

All these calculations indicate that the fatigue fracture of the longeron was initiated as a result of high stress concentration in the corrosion-cracking site and not because of an overloading event.

One can see that, regarding the levels of equivalent stresses, the longeron sections at the \bar{R} -value 0.7 and 0.5 are close to one another; this finding is consistent with the data on crack-growth durations and stress levels calculated for longerons. In the discussed longeron, initial corrosion cracking (intergranular) reached 0.4-mm depth. Then in 5-mm distance predominantly corrosion cracking (transgranular and intergranular) transformed to purely fatigue cracking (transgranular). Next to this zone, fatigue crack propagated for quite a long period. Here, the value of equivalent stress did not exceed the designed level. Therefore, fatigue crack would not nucleate without stress concentration, caused by the corrosion cracking deeper than 0.3 mm from the outer surface of the longeron, as long as the surface layer of such thickness experiences the residual compression stresses greater than the equivalent tensile stress.

The monitoring system employed to watch the longeron impermeability of the Mi-family helicopters is efficient.

CONCLUSION

- In cases of nucleation and propagation of fatigue cracks in the longerons of Mi-4 and Mi-8 helicopters in-service stresses never exceeded the designed levels at any relative radius of the propeller blades
- the longest crack-growth periods are typical of the basement part of the blades
- through fatigue cracks show the growth periods of tens flights for a whichever relative radius of a propeller blade; hence, such cracks can be revealed in good time with the pressure gages, installed in the blades to signal about the loss of their impermeability.

REFERENCES

- [1] Shanyavskiy, A.A., Tolerance fatigue cracking of aircraft structures. *Synergetics in engineering applications*. Monograph, Ufa (Russia), (2003)
- [2] Shanyavskiy A.A., Quantitative fractographic analyses of fatigue crack growth in longerons of in-service helicopter rotor-blades. *Fatigue Fract. Engng Mater Struc.*, 19 (1996) 1129-1141.
- [3] Shanyavskiy A.A., Toushentsov A.L., Effectiveness of safety flight guaranty for helicopters using introduced in longeron rotor-blade device for cracks detecting. Science Works for Investigators Society of Crashed Aircrafts, Russia, 11 (1999) 110-128.
- [4] Shanyavskiy A.A., Orlov E.F., Koronov M.Z., Fractographic analyses of fatigue crack growth in D16T alloy subjected to biaxial cyclic loads at various R-ratios. *Fatigue Fract. Engng Mater Struc.*, 18 (1995) 1263-1276.
- [5] Shanyavskiy A.A., Orlov E.F., Grigoriev V.M., Fatigue crack growth in D16 Al-alloy sheet subjected to biaxial out-of-phase loading. *Fatigue Fract. Engng Mater Struc.*, 20 (1997) 975-983.
- [6] Chan K.S., Hack L.E., Leverat G.R. Fatigue crack propagation in Ni-base superalloy single crystals under multiaxial cyclic loads. *Met. Trans.* 17A (1986) 1739-1750.
- [7] Murakami, Y. (Ed.) *Stress Intensity Factors Handbook* (in 3 volumes), Pergamon Press, Oxford, (1987).